Available online at www.sciencedirect.com

ScienceDirect

Mendeleev Commun., 2021, **31**, 224–226

Mendeleev Communications

Mechanism of the platinum nanoparticles formation under conditions of nonstationary electrolysis

Alexandra B. Kuriganova,* Mikhail S. Lipkin and Nina V. Smirnova

Platov South Russian State Polytechnic University (NPI), 346428 Novocherkassk, Russian Federation.
E-mail: kuriganova_@mail.ru

DOI: 10.1016/j.mencom.2021.03.026

The cathodic polarization of platinum in both aqueous and non-aqueous alkali metal ion electrolytes includes electrochemical adsorption of solvent molecules as well as intercalation of the alkali metal ions into an adsorption layer. The intercalation into oxidized platinum surface proceeds more effective compared with pure platinum.

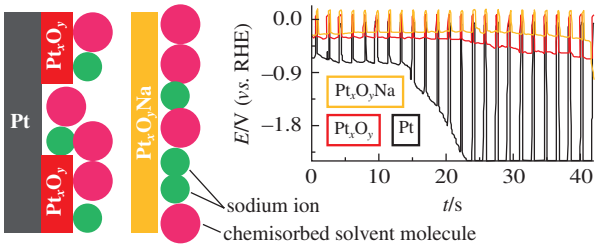

Keywords: platinum, acetonitrile, electrochemical dispersion, nonstationary electrolysis, intermetallic compound, potential step chronocoulometry, pulse chronopotentiometry.

Hydrogen energy technologies and in particular hydrogen fuel cell ones are regarded as advanced power sources with increasing commercial application.[1,2] However, the development of the corresponding market is hindered by the cost of fuel cell power plants with platinum catalysts as the most expensive components, on which the oxidation of hydrogen takes place. Thus, optimization of synthetic procedures for Pt-based catalysts represents a promising task. The known methods for production of Pt–C electrocatalysts typically include the formation of platinum nanostructures *via* chemical reduction of their precursors by reducing agents, which can simultaneously represent solvents, as in the polyol process,[3] and less frequently *via* high-energy ball milling[4] or atomic layer deposition,[5] with certain limitations being inherent to all the approaches. For example, the reduction methods typically consist of several steps and are highly sensitive to external factors. Therefore, special attention is drawn to methods of electrochemical origin for the production of Pt–C catalysts. In particular, the electrochemical dispersion technique has been developed for Pt electrodes under the influence of pulse alternating current, which leads to generation of platinum nanoparticles and their simultaneous deposition on a carbon support.[6,7] A mechanism was proposed in our work for the dispersion of Pt in an alkaline electrolyte, which was based on the intercalation of alkali metal from aqueous solution into the platinum surface.[8] This process was shown to include (i) discharge and cathodic insertion of alkali metal cations into the Pt lattice, (ii) decomposition of the platinum–alkali metal intermetallic compound in reaction with water, (iii) electrochemical injection of vacancies from the metal bulk to the surface, (iv) evolution of hydrogen and oxygen according to the direction of alternating current, with formation and growth of an oxide on the Pt surface during the anodic period as well as reduction of the oxide upon its interaction with adsorbed molecular hydrogen during the cathodic one, (v) thermokinetic phenomena at the electrode–electrolyte interface as well as (vi) nucleation/growth of elementary cracks due to absorption of zero- and one-dimensional defects.

In this work, to confirm this mechanism in detail, we explored the alkali metals intercalation into platinum electrodes from aqueous and nonaqueous solutions using potential step chronocoulometry and pulse chronopotentiometry with Pt electrodes prepared by the approved technique.[†]

It is known that in metals with a close-packed structure an intercalation is possible only in the presence of structural defects such as vacancies, dislocations or intergranular boundaries.[9] The equilibrium concentration of vacancies in Pt metal is reported to be negligible.[10] Probably, this explains the low rate of platinum dispersion during cathodic polarization using direct current. However, the concentration of structural defects on the surface is much higher as confirmed by SEM images of the Pt surface before and after the electrochemical processing [Figure 1(*a*,*b*)].

It has been found that the accumulation rate of dispersed platinum increases significantly when pulsed alternating current is applied[8] and potential higher than 5 V is reached during the anode pulse

[†] In potential-step chronocoulometry, the test sample was polarized with a stepwise potential change $\Delta E = 0.04$ V at pulse duration 15 s. As a result, the current density dependence $j = f(t)$ was obtained and integrated for each stage. To the discrete function for the charge passed *vs.* potential $Q = f(E)$, differentiation with preliminary spline interpolation was applied. For the correct determination of desired derivative, the spline approximation of the initial dependence $E = f(\log Q)$, differentiation of the obtained spline and calculation of reciprocal of the resulting derivative were performed.

Pulse measurements were carried out with a three-electrode clamp type sensor including an Ag/AgCl reference electrode and a carbon fiber counter electrode, using a P-45X potentiostat (Elins, Russia). Potentials are expressed relative to a reversible hydrogen electrode (RHE) for aqueous solutions and an Ag/AgCl electrode for the acetonitrile ones.

Pt electrodes were etched in nitric acid, rinsed repeatedly with double distilled water, polished with aluminum powder and again rinsed with water.

SEM investigations of the platinum electrodes before and after the electrochemical dispersion procedure were performed using a Quanta 200 microscope (FEI). TEM images were obtained employing a JEM-2100 microscope (JEOL).

XRD analysis and the crystallite size determination were carried out using an ARL X'TRA powder diffractometer (Thermo Scientific) at λ(CuKα) = 1.5418 Å and 2θ range of 20–80° with step scan mode at step width 0.01° and step time 2.00 s.

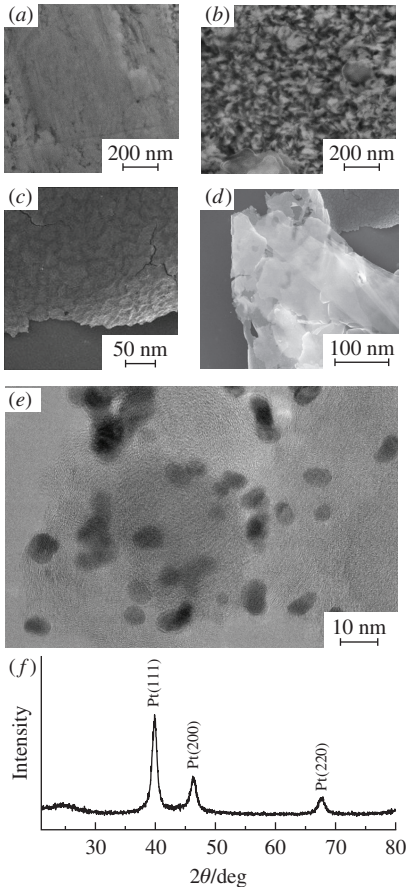

Figure 1 SEM images of the Pt electrode surface (*a*) before and (*b*) after the electrochemical processing. (*c*,*d*) SEM images of the platinum oxide film. (*e*) TEM image of Pt nanoparticles deposited onto Vulcan XC-72 carbon black. (*f*) XRD pattern for the Pt nanoparticles.

period. At even higher potentials, when the Pt electrode is dispersed in the electrolyte volume, partial oxidation of Pt particles is possible[11] due to formation of various chemisorbed oxygen species and the phase of platinum oxide,[12,13] and the presence of the latter facilitates the intercalation of alkali metal ions into the sorption layer. As follows from the two different SEM images of the Pt oxide film, it has uneven thickness [Figure 1(*c*,*d*)]. X-ray microanalysis revealed that the film had the known composition Pt_xO_yNa, where $x = 1–1.5$ and $y = 3–3.5$.[8] Platinum nanoparticles were formed as a result of the application of alternating pulsed current to Pt electrodes in an aqueous electrolyte with an alkali metal cation [Figure 1(*e*)]. The particles size along the (111) direction was determined to be 10.6 nm from XRD data [Figure 1(*f*)] using the Scherrer equation.

Chronopotentiometry was employed to obtain the dependence potential *vs.* time during the polarization of electrode by the current pulses with the constant or uniformly increasing current amplitude. The resulting function represents a combination of constant current chronopotentiograms and the potential decay curves after a current cutoff, which allows to estimate the instantaneous potential under current E_j and the instantaneous open circuit potential (IOCP), the latter represents the value of potential at the time of the end of a pause. The difference between these potentials is an estimate of instantaneous polarization. The obtained pulse chronopotentiograms were used in two different polarization modes to evaluate the intercalation capacity that made up the potential value (mode 1) and to calculate the transition time τ for each pulse (mode 2). The latter parameter represents an interval during which the entire reagent in the near-electrode region is completely consumed, which at constant current density and reagent concentration is proportional to the corresponding diffusion coefficient.

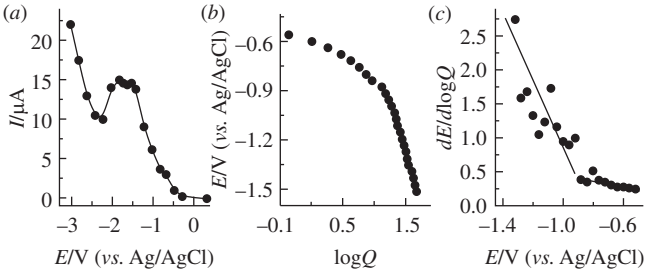

Figure 2 Voltammetry data of a Pt electrode in 1 M solution of $LiBF_4$ in acetonitrile: (*a*) cathodic polarization at sweep rate of 4 mV s^{-1}, (*b*) IOCP (see the text) *vs.* logarithm of the charge passed when expressed in μC and (*c*) $dE/d\log Q$ *vs.* the IOCP value.

Considering the intercalation phenomena, deviation from the classical Sand equation may originate from the difference of potential function from the Nernst model. In this regard, the transition time τ was found from the following equation for the potential *vs.* time:

$$E(t) = A + D\ln[(\sqrt{\tau}-\sqrt{t})/\sqrt{\tau}], \quad (1)$$

where the parameters A and D were calculated using the known Levenberg–Marquardt algorithm.[14]

For 1 M solution of $LiBF_4$ in acetonitrile, the conventional voltammetric dependence is characterized by a maximum current at the platinum electrode potentials $E = –1.5$ to $–1.9$ V and an implicit flattening platform at $E = –0.9$ to $–0.7$ V *vs.* Ag/AgCl [Figure 2(*a*)]. Taking into account the electrochemical inertness of acetonitrile in the E range employed, the observed singular points can be assigned to the cathodic incorporation of lithium. High values of the intercalation potentials indicate the inclusion into surface species formed by the solvent molecules rather than into the bulk platinum metal.

The presence a chemisorption layer of acetonitrile on the platinum surface was proved by the weak dependence of capacitance of double electric layer of the electrode on its potential in the presence of Et_4NClO_4.[15] The occurrence of acetonitrile chemisorption also coincides with the known *in situ* IR spectroscopic data on single crystal platinum surface in the same electrolytes.[16] At potentials more positive than the zero charge potential, the chemisorption originates from the lone electron pair of the nitrogen atom, while at more negative potentials, a hybridization type changes and the acetonitrile molecules are reoriented in the chemisorption layer. The accumulation of solvated cations in the double electric layer was also detected. Thus, an implicit bend of the curve at *E ca.* –0.9 V [Figure 2(*b*,*c*)] corresponds to adsorption of solvent molecules and the formation of adsorption layer, after which lithium ion intercalates into the layer. Thus, the significant difference between the intercalation potential and the potential region prevailing for the formation of alloys, namely –2.5 to –3.0 V *vs.* Ag/AgCl in acetonitrile, can be explained. The minimum at *ca.* –2.2 V [see Figure 2(*a*)] apparently results from saturation of the adsorption layer. Only in the range of potentials less than –2.3 V does lithium intercalate into the deep layers of the platinum metal and then becomes electrodeposited.

Pulse chronopotentiograms of platinum in the acetonitrile electrolyte demonstrate a horizontal section of considerable length in the IOCP values range of –0.6 to –0.8 V (*vs.* Ag/AgCl) [Figure 3(*a*,*b*)], the end of which corresponds to the formation of a saturated chemisorption layer.

The chronopotentiograms of platinum electrode in aqueous solutions [Figure 3(*c*,*d*)] reveal the following. The potential *vs.* time dependence for 2 M NaOH solution is characterized by nearly constant IOCP value of *ca.* –0.2 V, which is apparently determined by the redox pair of hydrogen [see Figure 3(*d*)]. The polarization E_j describes a curve with a horizontal section at

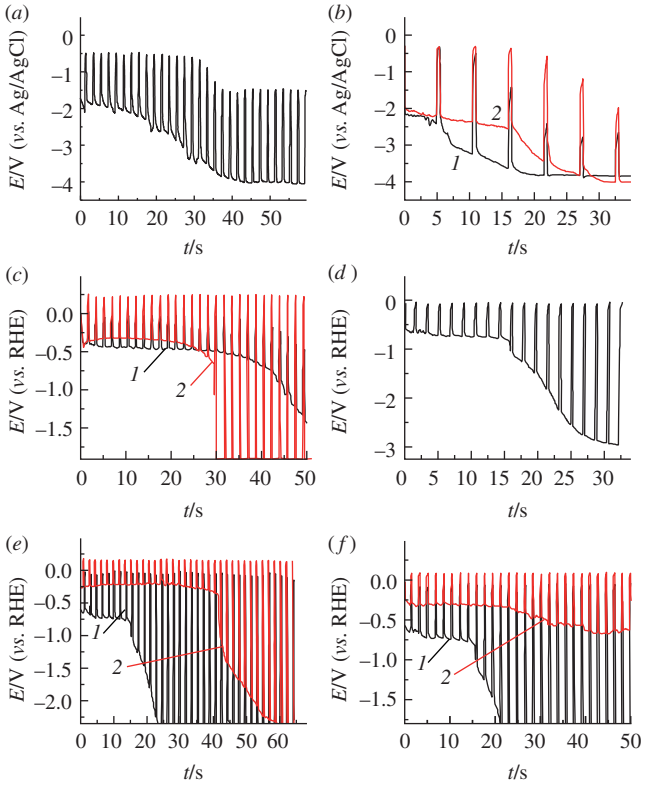

Figure 3 Pulse chronopotentiograms of (*a*) Pt in 1 M solution of $LiBF_4$ in acetonitrile (mode 1, see the text) without anodic polarization, (*b*) Pt in 1 M solution of $LiBF_4$ in acetonitrile (mode 2) (*1*) without polarization and (*2*) after the anodic polarization in 2 M aqueous NaOH solution at 3.2 V for 2 h, (*c*) Pt in 1 M aqueous LiOH solution (*1*) without polarization and (*2*) after the anodic polarization in 2 M aqueous NaOH solution at 3.2 V for 2 h, (*d*) Pt in 2 M aqueous NaOH solution, (*e*) (*1*) Pt and (*2*) Pt_xO_yNa film, both in 2 M aqueous NaOH solution, (*f*) (*1*) Pt_xO_yNa film and (*2*) Pt anodically oxidized in 2 M aqueous NaOH solution at 3.2 V for 2 h, both in 2 M aqueous NaOH solution.

–0.7 V, which is typical of intercalation. The inclusion of an alkali metal is confirmed in general by the dependence of the cathodic chronopotentiogram type on the nature of the metal cation. Thus, in the LiOH solution the potential range allowing to introduce lithium cations into platinum is significantly higher (E_j = –0.5 V), besides, the duration of the corresponding part of the curve, and hence the intercalation capacity of lithium ions, is more [see Figure 3(*c*)].

The intercalation capacity of anodically oxidized platinum is higher than the capacity of Pt_xO_yNa film (x = 1.0–1.5, y = 3.0–3.5) formed on the platinum electrode during polarization with an alternating pulse current of 0.02 mA cm^{-2} in 2 M aqueous NaOH solution [Figure 3(*e*, *f*)]. Apparently, with potential fluctuation in the range of 1.0–1.4 V on Pt in aqueous NaOH, the conditions are formed for the generation of platinum oxide film containing sodium, therefore, its alkali metal capacity is lower than that for the oxide phase formed at higher potentials [see Figure 3(*c*, *f*), curve *2*]. The IOCP value for oxidized Pt surface lies at 0.1–0.2 V larger anode potentials than for the unoxidized one. Thus,

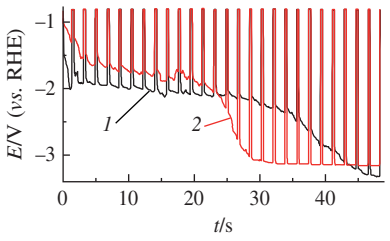

Figure 4 Pulse chronopotentiograms of Pt polarization in 1 M aqueous $LiBF_4$ solution as a neutral electrolyte: (*1*) without polarization and (*2*) after the anodic polarization in 2 M aqueous NaOH solution at 3.2 V for 2 h.

in aqueous solutions the IOCP value for the unoxidized platinum surface is determined by the reaction of hydrogen evolution, while for the oxidized one it is defined by the reduction of oxide film. On the other hand, polarization is determined by both the evolution of hydrogen and the presence of an alkali metal in the layer of chemisorbed solvent.

In 1 M solution of $LiBF_4$ as a neutral electrolyte, the cathodic pulsed chronopotentiogram (Figure 4, curve *1*) is characterized by significant polarization, which can be associated with kinetic hindrance of the lithium intercalation from its hydrated state in the absence of hydroxide ion. The values of IOCP under these conditions are nearly constant and determined, as for an alkaline electrolyte, by the hydrogen evolution reaction. After preliminary anodic polarization of platinum, the horizontal plot of the chronopotentiogram (Figure 4, curve *2*) moves to more positive potentials. However, the effect of the preliminary anodic polarization is weaker in neutral electrolyte than in acetonitrile [see Figure 3(*a*)] or alkaline electrolytes [see Figure 3(*c*, *f*)].

In summary, the cathodic polarization of platinum in aqueous (alkaline and neutral) as well as nonaqueous electrolytes includes electrochemical adsorption of solvent molecules and intercalation of alkali metal ions into the adsorption layer. The intercalation from aqueous solutions is activated by hydroxide ions, the corresponding capacity for lithium and sodium cations being different. In the presence of surface oxides on platinum, the intercalation into the adsorption layer is facilitated. The data on the behaviour of the Pt electrode in acetonitrile and aqueous solutions with alkali metal cations using the pulsed methods confirms the possibility of cathodic incorporation of the alkali metals into platinum at E < –1.7 V. It was also demonstrated that in the presence of chemisorbed oxygen or oxide phase on Pt, the intercalation was facilitated and observed even at E < –1.3 V. With polarization by pulsed alternating current during the cathode pulse, potentials are significantly lower ($E \leqslant$ –1.5 V), which creates conditions favourable for the intercalation of alkali metals into platinum.

This work was supported by the Russian Science Foundation (grant no. 20-79-10063).

References

1 Z. F. Pan, L. An and C. Y. Wen, *Appl. Energy*, 2019, **240**, 473.
2 I. Staffell, D. Scamman, A. Velazquez Abad, P. Balcombe, P. E. Dodds, P. Ekins, N. Shah and K. R. Ward, *Energy Environ. Sci.*, 2019, **12**, 463.
3 J. Chen, T. Herricks and Y. Xia, *Angew. Chem., Int. Ed.*, 2005, **44**, 2589.
4 M. Lucariello, N. Penazzi, E. Arca, G. Mulas and S. Enzo, *Mater. Chem. Phys.*, 2009, **114**, 227.
5 V. Miikkulainen, M. Leskelä, M. Ritala and R. L. Puurunen, *J. Appl. Phys.*, 2013, **113**, 021301.
6 K. Novikova, A. Kuriganova, I. Leontyev, E. Gerasimova, O. Maslova, A. Rakhmatullin, N. Smirnova and Y. A. Dobrovolsky, *Electrocatalysis*, 2018, **9**, 22.
7 A. B. Kuriganova, I. N. Leontyev, A. A. Ulyankina and N. V. Smirnova, *Mendeleev Commun.*, 2020, **30**, 663.
8 A. B. Kuriganova, D. V. Leontyeva and N. V. Smirnova, *Russ. Chem. Bull., Int. Ed.*, 2015, **64**, 2769 (*Izv. Akad. Nauk, Ser. Khim.*, 2015, 2769).
9 B. N. Kabanov, I. I. Astakhov and I. G. Kiseleva, *Electrochim. Acta*, 1979, **24**, 167.
10 Y. Kraftmakher, *Phys. Rep.*, 1998, **299**, 79.
11 D. E. Doronkin, A. B. Kuriganova, I. N. Leontyev, S. Baier, H. Lichtenberg, N. V. Smirnova and J.-D. Grunwaldt, *Catal. Lett.*, 2016, **146**, 452.
12 B. E. Conway, *Prog. Surf. Sci.*, 1995, **49**, 331.
13 N. Cabrera and N. F. Mott, *Rep. Prog. Phys.*, 1949, **12**, 163.
14 P. Wilson and H. A. Mantooth, *Model-Based Engineering for Complex Electronic Systems*, 1st edn., Newnes, 2013.
15 O. A. Petrii and I. G. Khomchenko, *J. Electroanal. Chem. Interfacial Electrochem.*, 1980, **106**, 277.
16 N. S. Marinković, M. Hecht, J. S. Loring and W. R. Fawcett, *Electrochim. Acta*, 1996, **41**, 641.

Received: 16th September 2020; 20/6313